

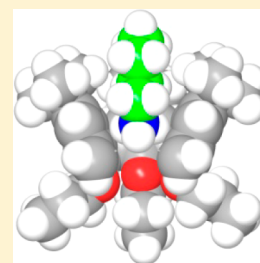
Endo-Complexation of Alkylammonium Ions by Calix[4]arene Cavity: Facilitating Cation- π Interactions through the Weakly Coordinating Anion Approach

Carmen Talotta,* Carmine Gaeta, and Placido Neri*

Dipartimento di Chimica e Biologia, Università di Salerno, Via Giovanni Paolo II 132, I-84084 Fisciano, Salerno, Italy

S Supporting Information

ABSTRACT: Notwithstanding its small dimensions, the narrow cavity of *p*-*tert*-butylcalix[4]arene macrocycle is still able to host alkylammonium guests in the presence of the tetrakis[3,5-bis(trifluoromethyl)phenyl]borate (TFPB⁻) weakly coordinating (or “superweak”) anion. As an artificial analogue of biological receptors, cone-shaped calix[4]arene **1d** is able to recognize a *n*-BuNH₃⁺ guest mainly through a 4-fold cation- π interaction aided by a weak H-bonding interaction. This recognition motif can be used to assembly a 2:1 capsular architecture with a linear diammonium axle.



Molecular recognition¹ is one of the fundamental and significant processes in living systems and in this context the knowledge of the secondary interactions at the base of the substrate/receptor stabilization is of crucial importance for the design of new drugs. In recent years, several studies have established that secondary interactions such as hydrogen bonds² and cation- π ³ interactions play a special role in many biological recognition processes. In a fundamental work, Xiu and Puskar^{4a} have showed that the high affinity of nicotine to $\alpha 4\beta 2$ neuronal receptor is due to a cation- π interaction between the positively charged nicotine ⁺NH and the aromatic ring of the TrpB (residue 149) in the receptor binding site (Figure 1, left). In addition, a hydrogen-bonding interaction

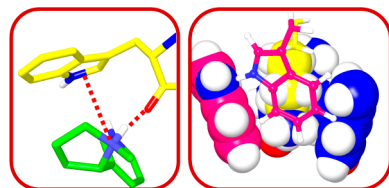


Figure 1. (Left) Particular of the interaction of nicotine (green) with the TrpB residue (yellow) in the X-ray structure of the complex between nicotine and acetylcholine binding protein (ACHBP).^{4b} (Right) Particular of the 4-fold cation- π interaction observed in the glucoamylase X-ray structure between the ammonium cation of Lys-108 (yellow) residue and the aromatic walls of Trp (magenta) and Tyr (blue) residues.⁵

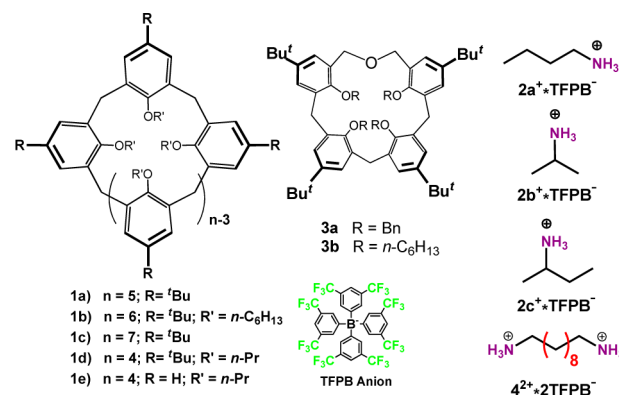
between the ⁺NH donor group of the substrate and the carbonyl group of TrpB (Figure 1, left) contributes to stabilize the complex.^{4b} An analogous action mode has been proposed for the binding of the smoking cessation drug cytosine in the same receptor site.^{4c} Interestingly, a 4-fold cation- π interaction (Figure 1, right) has been observed in a glucoamylase X-ray

structure between the ammonium cation of Lys-108 and the four π -electron-rich aromatic walls of Trp-120, Trp-52, Tyr-50, and Tyr-116.⁵

Inspired by the biological recognition motifs for the charged ammonium substrates,⁶ the design and development of artificial ammonium receptors represent a fascinating area of research in supramolecular chemistry. Consequently, a particular attention has been devoted to the recognition of ammonium guests by macrocycles such as calixarenes,⁷ pillarenes,⁸ crown ethers,⁹ and cucurbiturils.¹⁰

Regarding the calixarene macrocycles, Pappalardo and Parisi reported the first examples in which a preformed 20-membered calix[5]arene cavity **1a** (Chart 1) was exploited for the *endo*-cavity complexation of linear alkylammonium guests.^{7b-d} Successively, we have obtained the first examples of *endo*-cavity complexation of large calix[6,7]arene macrocycles^{7g,h} **1b,c** (24-

Chart 1



Received: July 23, 2014

Published: September 12, 2014

and 28-membered, respectively) with alkylammonium organic cations $2a-c^+$ by exploiting the inducing effect of the weakly coordinating (or “superweak”) anion tetrakis[3,5-bis-(trifluoromethyl)phenyl]borate (TFPB⁻). More recently, we have shown that the 18-membered dihomooxalix[4]arene macrocyclic **3a,b** is currently the smallest calixarene able to host linear and branched alkylammonium guests inside its aromatic cavity.⁷¹ Notwithstanding that the calix[4]arene macrocycle is the most popular and studied among all congeners, strangely, no examples of such complexation by its 16-membered macrocyclic **1d** have been so far reported. This is probably attributable to a diffuse conviction that its cavity is too small to host alkylammonium ions.

Thus, in order to clarify if the narrow cavity of the calix[4]arene macrocycle can or cannot be able to host alkylammonium guests, we decided to study the molecular recognition properties of tetrapropoxy-*p*-*tert*-butylcalix[4]arene **1d** toward alkylammonium ions $2a-c^+$ (Chart 1), and we wish to report here the results of these studies. Initially, we decided to test the complexing abilities of conformationally blocked cone-shaped **1d** toward the primary, linear *n*-butylammonium guest $2a^+$ (Chart 1). Unexpectedly, ¹H NMR experiments at room temperature (Figure 2) evidenced clear complexing

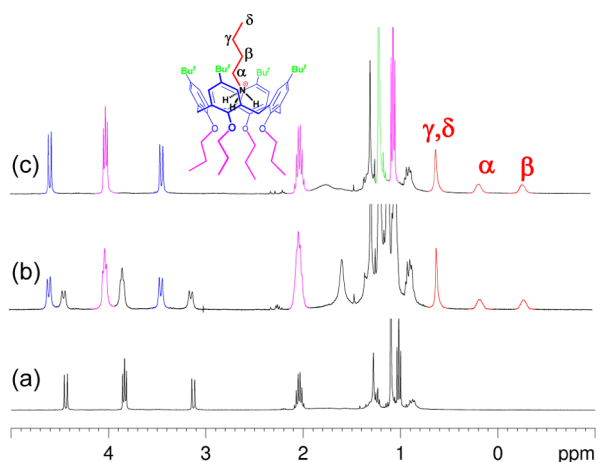


Figure 2. Significant portion of the ¹H NMR spectra (CDCl₃, 400 MHz, 298 K) of (a) **1d** (3 mM), (b) **1d** (3 mM) after the addition of 0.5 equiv of *n*-BuNH₃⁺·TFPB⁻, (c) equimolar mixture of **1d** (3 mM) and *n*-BuNH₃⁺·TFPB⁻. The coloring of the signals corresponds to that used in the *n*-BuNH₃⁺·**1d** structure drawing.

properties of **1d** toward TFPB⁻ salt of $2a^+$. In fact, after the addition of $2a^+$ ·TFPB⁻ to a CDCl₃ solution of **1d**, a new set of signal emerged in its ¹H NMR spectrum (Figure 2)¹¹ due to the formation of the *n*-BuNH₃⁺·**1d** complex (structure drawing in Figure 2) slowly exchanging in the NMR time scale. Diagnostic of the *endo*-cavity disposition of $2a^+$ is the presence of *n*-butyl resonances in the negative upfield region of the spectrum (Figure 2). In accord with this proposed model, a 2D ROESY¹¹ experiment showed ROE correlations among the shielded α and β signals of $2a^+$ and the aromatic protons of **1d** at 7.21 ppm (Figure S6, Supporting Information). In addition, complex formation was also confirmed by an ESI(+) mass spectrum¹¹ (Figure S3, Supporting Information) which gave as the base peak a value of 892.18 *m/z* corresponding to the supramolecular ion *n*-BuNH₃⁺·**1d**. In addition, the complete assignment of all *n*-BuNH₃⁺ resonances was carried out by means of a COSY-45 spectrum: α 0.20 ppm, β -0.28 ppm, γ

0.61 ppm, and δ 0.61 ppm (Figure S5, Supporting Information).¹¹

In this way, it was clear that the *n*-butyl protons that experience the highest complexation-induced shift (CIS) are those at the α position which undergo an upfield shift of 2.75 ppm, while the protons at β , γ , and δ position experience a CIS of 1.79, 0.71, and 0.29 ppm, respectively. Interestingly, the upfield shift experienced by α protons of guest $2a^+$ (2.75 ppm) is significantly lower than that previously observed for its analogous *endo*-complex with dihomooxalix[4]arene **3a**⁷¹ (3.84 ppm) or calix[5]arene **1a**^{7c} (3.87 ppm). In addition, it is also lower with respect to that obtained with larger calix[6]arene macrocycle **1b**^{7b} (2.89 ppm). Analogously, β , γ , and δ protons of $2a^+$ also experience a CIS significantly lower to that previously observed for its analogous *endo*-complexation with **3a**, **1a**, and **1b**. Therefore, the CIS and ROESY data clearly indicates that the penetration of *n*-butylammonium guest $2a^+$ is less deeper in the narrow calix[4]arene cavity of **1d** with respect to all the other larger cavities of hosts **3a**, **1a**, and **1b**.

This binding mode was confirmed by the lowest energy structure of the complex (Figure 3a–c, DFT calculations¹² at

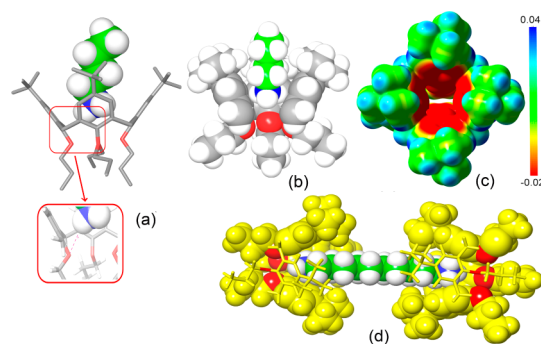


Figure 3. Optimized structures of *n*-BuNH₃⁺·**1d** (a) and 4^{2+} ·**C(1d)₂** (d) complexes at the B3LYP/6-31G* level of theory. (b) Particular showing the close proximity between the positive ammonium center of $2a^+$ and the aromatic walls of **1d** to give cation- π interactions (the frontal aromatic ring of **1d** has been omitted for clarity). (c) ESP mapped onto electron density isosurface ($\rho = 0.005 \text{ e/au}^3$) for **1d**.

the B3LYP/6-31G* level of theory) where it is possible to measure a distance of 3.28 Å between the N-atom of $2a^+$ and the mean plane of the lower rim oxygens of **1d**, which is significantly higher than that observed for the analogous complex with dihomooxalix[4]arene **3a**⁷¹ (1.48 Å) and calix[6]arene **1b**^{7b} (0.76 Å).

A close inspection of the optimized structure (Figure 3a,b) revealed an average distance of 3.9 Å between the nitrogen atom of $2a^+$ and the centroid of the aromatic rings of **1d**, a value very similar to that observed (4.3 Å) in the nicotine/ACHBP complex (Figure 1, left). A further scrutiny of the BuNH₃⁺·**1d** structure evidenced the presence of one hydrogen bond between one ammonium proton of $2a^+$ and a lower rim oxygen of **1d** with a N⁺⋯O distance of 3.9 Å (Figure 3a), which is indicative of a weak interaction. Thus, calix[4]arene **1d** can be considered an artificial analogue of the ACHBP receptor, since it is able to recognize *n*-BuNH₃⁺ guest through cation- π interactions,³ between the positive nitrogen atom of $2a^+$ and the Ar rings of **1d** and through a weak H-bonding interaction between NH⁺ and OR groups. From another point of view, the encasing of *n*-BuNH₃⁺ ion within the four aromatic walls of **1d**

is very similar to the 4-fold cation– π interaction observed in a glucoamylase X-ray structure (Figure 1, right).⁵

An apparent association constant of $2.69 \pm 0.5 \times 10^5 \text{ M}^{-1}$ was determined through a competition experiment (Figure S16, Supporting Information)^{13a} by treating 1 equiv of $2a^+ \cdot \text{TFPB}^-$ in CDCl_3 (1.5 mM) with a mixture of **1d** and **3a**⁷ⁱ (1 equiv each). Thus, it was evidenced that $2a^+ \cdot \text{C1d}$ is preferentially formed over $2a^+ \cdot \text{C1d}$ in a ratio of 15:1, probably thanks to the formation of two H-bonds between the ammonium H atoms of $2a^+$ and both O-atoms of the ethereal bridge and of the lower rim of dihomooxa macrocycle **3a**⁷ⁱ with respect to the formation of only one weak H-bond between $2a^+$ and **1d**. The apparent association constant observed for $2a^+ \cdot \text{C1d}$ complex ($2.69 \pm 0.5 \times 10^5 \text{ M}^{-1}$) was significantly lower than that observed for the analogous complexation of $2a^+$ with calix[6]arene **1b** host ($8.30 \times 10^6 \text{ M}^{-1}$).^{7g} Obviously, this lower affinity is attributable to the minor strength of cation– π interactions with respect to hydrogen bonds that mainly stabilize the two complexes, respectively.

In a seminal work, Dougherty and co-workers¹⁴ proposed the analysis of the electrostatic surface potential (ESP) of aromatic hosts as an useful guidelines for assessing cation– π interacting abilities in new systems. In accordance with this suggestion, we report the ESP (Figure 3d) of the calix cavity of **1d** generated by mapping the ESP onto a molecular surface corresponding to an isodensity contour at $\rho = 0.005 \text{ e/au}^3$. As expected, we found a sharp negative electrostatic potential (red region in Figure 3d) into the calix cavity, which is fully consistent with a strong electrostatic attraction toward the positively charged ammonium ion.

In order to evaluate the influence of the TFPB superweak anion in the $n\text{-BuNH}_3^+$ complexation by **1d**, we decided to perform similar studies in the presence of different anions such as Cl^- and PF_6^- (Figure S15, Supporting Information). Not surprisingly, in all these instances no appreciable interactions could be detected, thus confirming the fundamental role of TFPB^- in the ion-pair separation,¹⁵ which allows the establishment of otherwise impossible cation– π interactions. Therefore, the “superweak anion” approach can be considered a quite effective and general method to facilitate cation– π interactions in various systems.¹⁶

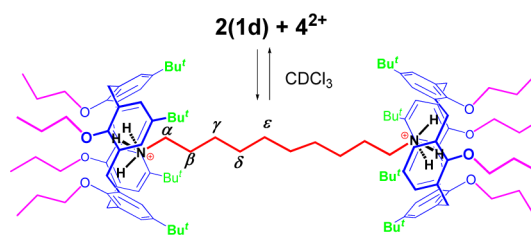
A further point worthy of consideration is the surprising slow exchange of $n\text{-BuNH}_3^+ \cdot \text{C1d}$ complex in the NMR time scale. This can be ascribed to the interdigitation of calixarene *t*-Bu groups with the *n*-Bu aliphatic chain, which gives rise to favorable van der Waals interactions. In accordance with this explanation, we found that the complexation of $n\text{-BuNH}_3^+$ by the *t*-Bu-depleted calix[4]arene **1e** is fast in the NMR time scale and is characterized by a lower apparent association constant ($540 \pm 40 \text{ M}^{-1}$).¹¹

Successively, we decided to extend the binding studies of calix[4]arene **1d** to branched alkylammonium guests **2b–c**⁺. Differently from the linear alkylammonium $2a^+$, the addition of *i*-PrNH₃⁺ guest **2b**⁺ (Chart 1) to a CDCl_3 solution of **1d** (400 MHz, 298 K) caused shifts of the host signals due to a fast complexation equilibrium in the NMR time scale (Figure S7, Supporting Information).¹¹ The ¹H NMR spectrum of an equimolar solution of **1d** and **2b**⁺ evidenced the presence of a shielded broad signal of *i*-PrNH₃⁺ guest at -0.37 ppm (Figure S7c, Supporting Information),¹¹ well compatible with an *endo*-cavity $2b^+ \cdot \text{C1d}$ complex formation. Analogous results were obtained for the *s*-BuNH₃⁺ guest **2c**⁺ (Figure S8, Supporting Information). An apparent association constant of 140 ± 20

and $90 \pm 15 \text{ M}^{-1}$ was determined for $2b^+ \cdot \text{C1d}$ and $2c^+ \cdot \text{C1d}$ complexes, respectively, by a nonlinear least-squares fitting procedure (EQNMR^{13b} program). Clearly, both values are significantly lower than that observed for $2a^+ \cdot \text{C1d}$ ($2.69 \pm 0.5 \times 10^5 \text{ M}^{-1}$) probably due to the larger dimensions of the branched guests **2b–c**⁺, which only allow the establishment of quite weaker cation– π interactions.

As a final point, on the basis of the formation of the slowly exchanging $n\text{-BuNH}_3^+ \cdot \text{C1d}$ complex, we decided to study the complexation of a linear α,ω -dialkylammonium ion by calix[4]arene **1d**. In analogy with what observed by Pappalardo and Parisi with calix[5]arene hosts,¹⁷ it could be expected that also in our case, in the presence of an appropriate guest length, a 2:1 capsular complex could be formed (Scheme 1). Taking advantage of the “molecular ruler” studies of Pappalardo and Parisi,¹⁷ we selected 1,10-diammoniumdecane **4**²⁺ as a suitable guest to this purpose.

Scheme 1. Self-Assembly of the Dimeric Capsular $4^{2+} \cdot \text{C}(\text{1d})_2$ Architecture



Thus, when the TFPB salt of dicationic **4**²⁺ was added to a CDCl_3 solution of **1d** (Scheme 1) a new set of signals emerged in the ¹H NMR spectrum (colored signals in Figure S10b, Supporting Information), due to the formation of a new species slowly exchanging in the NMR time scale. In particular, a typical signature was seen at highfield negative values (from 1.0 to -1.0 ppm), which is characteristic of the *endo*-complexation of the alkyl chains shielded by calixarene aromatic rings. An ESI(+) mass spectrum (Figure S11, Supporting Information) of the mixture gave a prominent peak at 897.45 m/z corresponding to a doubly charged supramolecular ion in which two calix[4]arene **1d** units are locked around the two terminal ammonium sites of **4**²⁺ to give the dimeric capsular architecture $4^{2+} \cdot \text{C}(\text{1d})_2$ (Scheme 1).¹¹ A COSY-45 spectrum of $4^+ \cdot \text{C}(\text{1d})_2$ complex (Figures S12–S13, Supporting Information) confirmed the double-*endo*-complexation and the consequent 2-fold molecular symmetry.¹¹ In fact, only four symmetry-related, scalar *J*-couplings were observed between α methylene protons (0.14 ppm) and their linked β protons (-0.31 ppm), which were coupled to γ protons (0.51 ppm), which in turn were coupled with δ protons (0.83 ppm) and finally coupled with ϵ methylene protons at 0.97 ppm. Finally, an apparent association constant of $260 \pm 20 \text{ M}^{-2}$ was determined for the $4^{2+} \cdot \text{C}(\text{1d})_2$ complex.

The formation of the $4^{2+} \cdot \text{C}(\text{1d})_2$ capsular dimeric complex was also investigated by DOSY NMR.^{11,19} In particular, three DOSY spectra (400 MHz, 298 K) registered under identical conditions for the free host **1d**, the 1:1 $2a^+ \cdot \text{C1d}$ complex, and the 2:1 $4^{2+} \cdot \text{C}(\text{1d})_2$ assembly, gave a diffusion coefficient of 6.4×10^{-10} , 5.5×10^{-10} , and $3.7 \times 10^{-10} \text{ m}^2/\text{s}$, respectively, in good agreement with their increasing size (Figure S14, Supporting Information).¹¹ Undoubtedly, the formation of the slowly exchanging 2:1 $4^{2+} \cdot \text{C}(\text{1d})_2$ complex is worthy of note

since it is mainly assembled through weak cation– π interactions.

The binding mode of two calixarenes **1d** around the diammonium sites of axle **4²⁺** was also studied by DFT calculations¹² at the B3LYP/6-31G* level of theory (Figure 3d). In analogy to the **2a⁺**–**1d** model, an average distance of 3.69 Å was found between the nitrogen atom of **2a⁺** and the centroids of the aromatic rings of **1d**. Also in this case, a weak H-bonding interaction between one ammonium proton and a lower rim oxygen of **1d** (N⁺...O distance of 3.9 Å) was evidenced.

In conclusion, we have here shown that the narrow cavity of *p*-*tert*-butylcalix[4]arene, the smallest member of the calixarene family, is still able to host alkylammonium guests in the presence of a superweak anion, notwithstanding its small dimensions. In particular, as an artificial analogue of the ACHBP receptor, a cone-shaped tetrapropoxycalix[4]arene, is able to recognize a *n*-BuNH₃⁺ guest mainly through the action of a 4-fold cation– π interaction with the aid of van der Waals and very weak H-bonding interactions. Surprisingly, this stabilization is sufficient for the assemblage of an higher-order 2:1 capsular architecture with a linear diammonium axle. These results provide a further example of the great potentialities of the “superweak anion approach” in supramolecular chemistry, which can probably find further applications in various other systems involving cation interactions.

■ EXPERIMENTAL SECTION

ESI(+)-MS measurements were performed on a triple quadrupole mass spectrometer equipped with electrospray ion source, using CHCl₃ as solvent. All chemicals were reagent grade and were used without further purification. Anhydrous solvents were used as purchased from the supplier. When necessary, compounds were dried in vacuo over CaCl₂. Reaction temperatures were measured externally. Reactions were monitored by TLC silica gel plates (0.25 mm) and visualized by UV light, or by spraying with H₂SO₄–Ce(SO₄)₂.

Derivatives **2a–c**, **1d,e**, and sodium tetrakis[3,5-bis-(trifluoromethyl)phenyl]borate were synthesized according to literature procedures.^{7g,i,20} NMR spectra were recorded on a 600 MHz spectrometer [600 (¹H) and 150 MHz (¹³C)], 400 MHz spectrometer [400 (¹H) and 100 MHz (¹³C)], or 300 MHz spectrometer [300 (¹H) and 75 MHz (¹³C)]. Chemical shifts are reported relative to the residual solvent peak (CHCl₃: δ 7.26, CDCl₃: δ 77.23; CD₃OH: δ 4.87, CD₃OD: δ 49.0). Standard pulse programs, provided by the manufacturer, were used for 2D COSY, 2D ROESY, and 2D DOSY experiments. Molecular modeling studies were performed with a combined use of the MacroModel-9/Maestro-4.1²¹ program and the Gaussian-09 software package.²² GaussianView 5.0.8W was used in the calculation of ESP of **1d** at B3LYP/6-31G* level. The input structure of **1d** for ESP calculation was optimized at B3LYP/6-31G* level of theory.

Synthesis of 4²⁺·2TFPB⁻. 1,10-Diaminodecane (1.0 g, 5.8 mmol) was dissolved in Et₂O (20 mL) at room temperature, and an aqueous solution of HCl (37% w/w, 1 mL) was added dropwise. The mixture was kept under stirring for 15 min until a white precipitate was formed. The solid was collected by filtration, washed with MeOH (10 mL) and CH₃CN (10 mL), and dried under vacuum to give the chlorohydrate derivative as a white solid (1.4 g, 5.7 mmol, 98%). The obtained derivative (0.1 g, 0.41 mmol) was dissolved in warm, dry MeOH (10 mL), and then a solution of sodium tetrakis[3,5-bis(trifluoromethyl)phenyl]borate (0.80 g, 0.90 mmol) in dry MeOH (20 mL) was added. The mixture was kept under stirring overnight in the dark. The solvent was removed, and deionized water was added, obtaining a brown precipitate that was filtered off and dried under vacuum for 24 h to give derivative **4²⁺·2TFPB⁻** (0.74 g, 95%).

¹H NMR (300 MHz, CD₃OD, 298 K): δ 1.38 (overlapped, 8H, Hd +He), 1.65 (broad, 4H, Hc), 2.45 (broad, 4H, Hb), 3.65 (broad, 4H,

Ha), 7.61 (overlapped, ArH^{TFPB}, 24 H). ¹³C NMR (75 MHz, CD₃OD, 298 K): δ 26.2, 27.5, 29.1, 29.3, 39.6, 116.7, 119.2, 122.9, 126.3, 128.6, 129.5, 130.0, 134.6, 135.2, 160.4, 161.3, 162.0, 162.7. Anal. Calcd for C₇₄H₅₀B₂F₄₈N₂: C, 46.76; H, 2.65. Found: C, 46.68; H, 2.73.

Preparation of *n*-BuNH₃⁺·1d** complex.** Calixarene derivative **1d** (1.2 × 10⁻³ mmol) was dissolved in 0.4 mL of CDCl₃ (3 mM solution). Then, tetrakis[3,5-bis(trifluoromethyl)phenyl]borate salt **2a⁺** (1.2 × 10⁻³ mmol) was added, and the mixture was stirred for 15 min at 40 °C. After cooling, the solution was transferred in a NMR tube for 1D and 2D NMR spectra acquisition.

Determination of *K*_{assoc} Value of *n*-BuNH₃⁺·1d** Complex by ¹H NMR Competition Experiment.** ¹H NMR competition experiments were performed by analysis of a 1:1:1 mixture of hosts **1d** (H_A) and **3a** (H_B) with guest **2a⁺** (G) (3.8 mM each one) in an NMR tube using CDCl₃ as the solvent. In particular, 1.92 × 10⁻³ mmol of **2a⁺**, **1d**, and **3a** was mixed in 0.5 mL of CDCl₃ (3.8 mM each one). The following equations were used:

$$K_{GCH_A} = \frac{[H_A G]}{[H_A][G]} \quad K_{GCH_B} = \frac{[H_B G]}{[H_B][G]}$$

$$K_{rel} = \frac{K_{GCH_A}}{K_{GCH_B}} = \frac{[H_A G][H_B][G]}{[H_B G][H_A][G]}$$

$$\frac{[H_A G]}{[H_B G]} = \frac{[H_B]}{[H_A]} \quad K_{rel} = \frac{K_{GCH_A}}{K_{GCH_B}} = \frac{[H_A G]^2}{[H_B G]^2}$$

The complex concentrations [H_AG] and [H_BG] were evaluated by integration of the ¹H NMR signals of the complexes.

Determination of *K*_{assoc} for **2b⁺·**1d**, **2c⁺**·**1d**, and **2a⁺**·**1e** Complexes by ¹H NMR Titration.** ¹H NMR titrations were performed at 298 K in CDCl₃. The host concentration (5 mM) was kept constant while the guest concentration was varied (from 0.5 mM to 50 mM). In all cases, the signals of the host were followed and the data were analyzed by a nonlinear regression analysis.^{13b}

Preparation of 4²⁺·(1d)₂ Dimeric Complex. Calixarene derivative **1d** (4.0 × 10⁻³ mmol) was dissolved in 0.4 mL of CDCl₃ (10 mM). Then, **4²⁺·TFPB⁻** (2.0 × 10⁻³ mmol, 5 mM) was added, and the mixture was stirred for 15 min at 40 °C. After cooling, the solution was transferred in a NMR tube for 1D and 2D NMR spectra acquisition.

■ ASSOCIATED CONTENT

§ Supporting Information

2D COSY, ROESY, and DOSY spectra, ¹H NMR titration experiments, and detailed results of the DFT calculations. This material is available free of charge via the Internet at <http://pubs.acs.org>.

■ AUTHOR INFORMATION

Corresponding Authors

*E-mail: ctalotta@unisa.it.

*E-mail: neri@unisa.it.

Notes

The authors declare no competing financial interest.

■ ACKNOWLEDGMENTS

We thank the Italian MIUR (PRIN 20109Z2XRJ_006) for financial support and the Centro di Tecnologie Integrate per la Salute (Project PONA3_00138), Università di Salerno, for the 600 MHz NMR instrumental time. Thanks are due to Dr. Patrizia Oliva and Dr. Patrizia Iannece for instrumental assistance.

REFERENCES

- (1) *Comprehensive Supramolecular Chemistry*; Atwood, J. L., Davies, J. E. D., Macnicol, D. D., Vogtle, F., Eds.; Pergamon Press: New York, 1996.
- (2) Jefferey, G. A. *An Introduction to Hydrogen Bonding*; Oxford University Press: Oxford, 1997.
- (3) (a) Dougherty, D. A. *Acc. Chem. Res.* **2013**, *46*, 885–893. (b) Ma, J. C.; Dougherty, D. A. *Chem. Rev.* **1997**, *97*, 1303–1324.
- (4) (a) Xiu, X.; Puskar, N. L.; Shanata, J. A. P.; Lester, H. A.; Dougherty, D. A. *Nature* **2009**, *458*, 534–538. (b) Celie, P. H.; Van Rossum-Fikkert, S. E.; Van Dijk, W. J.; Brejc, K.; Smit, A. B.; Sixma, T. K. *Neuron* **2004**, *41*, 907–914. (c) Tavares Da Silva, X.; Blum, A. P.; Nakamura, D. T.; Puskar, N. L.; Shanata, J. A. P.; Lester, H. A.; Dougherty, D. A. *J. Am. Chem. Soc.* **2012**, *134*, 11474–11480.
- (5) Aleshin, A. E.; Stoffer, B.; Firsov, L. M.; Svensson, B.; Honzatko, R. B. *Biochemistry* **1996**, *35*, 8319–8328.
- (6) For further examples, see: (a) Miles, T. F.; Bower, K. S.; Lester, H. A.; Dougherty, D. A. *ACS Chem. Neurosci.* **2012**, *3*, 753–760. (b) Duffy, N. H.; Lester, H. A.; Dougherty, D. A. *ACS Chem. Biol.* **2012**, *7*, 1738–1745.
- (7) For a comprehensive review on calixarene macrocycles, see: (a) Gutsche, C. D. *Calixarenes, An Introduction*; Royal Society of Chemistry: Cambridge, UK, 2008. For examples regarding the ammonium guest recognition, see: (b) Arnaud-Neu, F.; Fuangswasdi, S.; Notti, A.; Pappalardo, S.; Parisi, M. F. *Angew. Chem., Int. Ed. Engl.* **1998**, *37*, 112–114. (c) Parisi, M. F.; Pappalardo, S. *J. Org. Chem.* **1996**, *61*, 8724–8725. (d) Capici, C.; Cohen, Y.; D'Urso, A.; Gattuso, G.; Notti, A.; Pappalardo, A.; Pappalardo, S.; Parisi, M. F.; Purrello, R.; Slovak, S.; Villari, V. *Angew. Chem., Int. Ed.* **2011**, *50*, 11956–11961. (e) Capici, C.; Gattuso, G.; Notti, A.; Parisi, M. F.; Pappalardo, S.; Brancatelli, G.; Geremia, S. *J. Org. Chem.* **2012**, *77*, 9668–9675. (f) Coquière, D.; de la Lande, A.; Marti, S.; Parisel, O.; Prangé, T.; Reinaud, O. *Proc. Natl. Acad. Sci. U.S.A.* **2009**, *106*, 10449–10454. (g) Gaeta, C.; Troisi, F.; Neri, P. *Org. Lett.* **2010**, *12*, 2092–2095. (h) Gaeta, C.; Talotta, C.; Farina, F.; Camalli, M.; Campi, G.; Neri, P. *Chem.—Eur. J.* **2012**, *18*, 1219–1230. (i) Gaeta, C.; Talotta, C.; Farina, F.; Teixeira, F. A.; Marcos, P. A.; Ascenso, J. R.; Neri, P. *J. Org. Chem.* **2012**, *77*, 10285–10293. (j) Talotta, C.; Gaeta, C.; Qi, Z.; Schalley, C. A.; Neri, P. *Angew. Chem., Int. Ed.* **2013**, *52*, 7437–7441. (k) Gaeta, C.; Talotta, C.; Neri, P. *Chem. Commun.* **2014**, *50*, 9917–9920.
- (8) (a) Fan, J.; Chen, Y.; Cao, D.; Yang, Y.-W.; Jia, X.; Li, C. *RSC Adv.* **2014**, *4*, 4330–4333. (b) Li, C.; Shu, X.; Li, J.; Fan, J.; Chen, Z.; Weng, L.; Jia, X. *Org. Lett.* **2012**, *14*, 4126–4129.
- (9) Gokel, G. W. *Crown Ethers and Cryptands: Monographs in Supramolecular Chemistry*; The Royal Society of Chemistry: Cambridge, 1991.
- (10) (a) Lagona, J.; Mukhopadhyay, P.; Chakrabarti, S.; Isaacs, L. *Angew. Chem., Int. Ed.* **2005**, *44*, 4844–4870. (b) Tootoonchi, H. M.; Yi, S.; Kaifer, A. E. *J. Am. Chem. Soc.* **2013**, *135*, 10804–10809. (c) Kim, Y.; Kim, H.; Ko, Y. H.; Selvapalam, N.; Selvapalam, N.; Rekharsky, M. V.; Inouew, Y.; Kim, K. *Chem.—Eur. J.* **2009**, *15*, 6143–6151. (d) Mock, W.; Shih, N. Y. *J. Am. Chem. Soc.* **1986**, *51*, 4440–4446.
- (11) See the Supporting Information for further details.
- (12) DFT calculations were performed at the B3LYP level using the 6-31G* basis set for the entire system (GAUSSIAN 09 Software Package).
- (13) (a) Hirose, K. *Analytical Methods*. In *Analytical Methods in Supramolecular Chemistry*; Schalley, C. A., Eds.; WILEY-VCH: Weinheim, 2007; Chapter 2, pp 17–54. (b) Hynes, M. J. *J. Chem. Soc., Dalton Trans.* **1993**, 311–312.
- (14) Mecozzi, S.; West, A. P.; Dougherty, D. A. *Proc. Natl. Acad. Sci. U.S.A.* **1996**, *93*, 10566–10571.
- (15) In 2010, we first showed that the “superweak anion approach” is quite effective for the threading and *endo*-cavity complexation of larger calix[6,7]arene macrocycles with alkylammonium guests.^{7g–k} Successively, the “superweak anion approach” was also extended to crown-ethers (Chen, N.-C.; Chuang, C.-J.; Wang, L.-Y.; Lai, C.-C.; Chiu, S.-H. *Chem.—Eur. J.* **2012**, *18*, 1896–1890) and pillararenes^{8b} (Han, C.; Gao, L.; Yu, G.; Zhang, Z.; Dong, S.; Huang, F. *Eur. J. Org. Chem.*, **2013**, 2529–2532).
- (16) For other examples of counterion effects in supramolecular chemistry, see: Gasa, T. B.; Cory Valente, C.; Stoddart, J. F. *Chem. Soc. Rev.* **2011**, *40*, 57–78 and references cited therein.
- (17) For recent examples of calixarene/ammonium-based dimeric architectures, see: (a) Gattuso, G.; Notti, A.; Pappalardo, A.; Parisi, M. F.; Pisagatti, I.; Pappalardo, S.; Garozzo, D.; Messina, A.; Cohen, Y.; Slovak, S. *J. Org. Chem.* **2008**, *73*, 7280–7289. (b) Brancatelli, G.; Gattuso, G.; Geremia, S.; Notti, A.; Pappalardo, S.; Parisi, M. F.; Pisagatti, I. *Org. Lett.* **2014**, *16*, 2354–2357 and references cited therein.
- (18) Körner, S. K.; Tucci, F. C.; Rudkevich, D. M.; Heinz, T.; Rebek, J., Jr. *Chem.—Eur. J.* **2000**, *6*, 187–195.
- (19) Cohen, Y.; Avram, L.; Frish, L. *Angew. Chem., Int. Ed.* **2005**, *44*, 520–554.
- (20) (a) Nishida, H.; Takada, N.; Yoshimura, M.; Sonoda, T.; Kobayashi, H. *Bull. Chem. Soc. Jpn.* **1984**, *57*, 2600–2604. (b) Ikeda, A.; Nagasaki, T.; Araki, K.; Shinkai, S. *Tetrahedron* **1992**, *48*, 1059–1070.
- (21) Mohamadi, F.; Richards, N. G.; Guida, W. C.; Liskamp, R.; Lipton, M.; Caufield, C.; Chang, G.; Hendrickson, T.; Still, W. C. *J. Comput. Chem.* **1990**, *11*, 440–467.
- (22) Frisch, M. J.; Trucks, G. W.; Schlegel, H. B.; Scuseria, G. E.; Robb, M. A.; Cheeseman, J. R.; Scalmani, G.; Barone, V.; Mennucci, B.; Petersson, G. A.; Nakatsuji, H.; Caricato, M.; Li, X.; Hratchian, H. P.; Izmaylov, A. F.; Bloino, J.; Zheng, G.; Sonnenberg, J. L.; Hada, M.; Ehara, M.; Toyota, K.; Fukuda, R.; Hasegawa, J.; Ishida, M.; Nakajima, T.; Honda, Y.; Kitao, O.; Nakai, H.; Vreven, T.; Montgomery, J. A., Jr.; Peralta, J. E.; Ogliaro, F.; Bearpark, M.; Heyd, J. J.; Brothers, E.; Kudin, K. N.; Staroverov, V. N.; Kobayashi, R.; Normand, J.; Raghavachari, K.; Rendell, A.; Burant, J. C.; Iyengar, S. S.; Tomasi, J.; Cossi, M.; Rega, N.; Millam, J. M.; Klene, M.; Knox, J. E.; Cross, J. B.; Bakken, V.; Adamo, C.; Jaramillo, J.; Gomperts, R.; Stratmann, R. E.; Yazyev, O.; Austin, A. J.; Cammi, R.; Pomelli, C.; Ochterski, J. W.; Martin, R. L.; Morokuma, K.; Zakrzewski, V. G.; Voth, G. A.; Salvador, P.; Dannenberg, J. J.; Dapprich, S.; Daniels, A. D.; Farkas, Ö.; Foresman, J. B.; Ortiz, J. V.; Cioslowski, J.; Fox, D. J. *Gaussian, Inc.*: Wallingford, CT, 2009.